

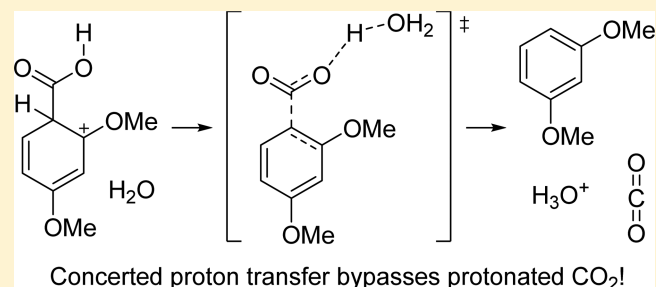
# How Acid-Catalyzed Decarboxylation of 2,4-Dimethoxybenzoic Acid Avoids Formation of Protonated CO<sub>2</sub>

Graeme W. Howe,<sup>†</sup> Adelle A. Vandersteen,<sup>†</sup> and Ronald Kluger\*<sup>‡</sup>

Davenport Chemical Laboratories, Department of Chemistry, University of Toronto, Toronto, Ontario M5S 3H6, Canada

**S** Supporting Information

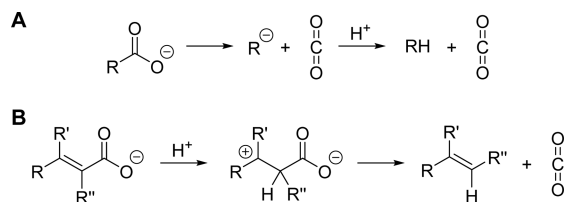
**ABSTRACT:** The decarboxylation of 2,4-dimethoxybenzoic acid (**1**) is accelerated in acidic solutions. The rate of reaction depends upon solution acidity in a manner that is consistent with the formation of the conjugate acid of **1** (RCO<sub>2</sub>H<sub>2</sub><sup>+</sup>), with its higher energy ring-protonated tautomer allowing the requisite C–C bond cleavage. However, this would produce the conjugate acid of CO<sub>2</sub>, a species that would be too energetic to form. Considerations of mechanisms that fit the observed rate law were supplemented with DFT calculations. Those results indicate that the lowest energy pathway from the ring-protonated reactive intermediate involves early proton transfer from the carboxyl group to water along with C–C bond cleavage, producing 1,3-dimethoxybenzene and CO<sub>2</sub> directly.



## INTRODUCTION

Decarboxylation reactions typically convert the conjugate base of a carboxylic acid to CO<sub>2</sub> and a stabilized carbanion or its functional equivalent (Scheme 1A).<sup>1,2</sup> A mechanistically

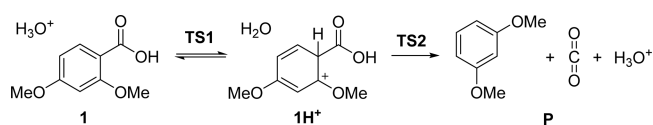
Scheme 1. Decarboxylation Can Occur by Formation of CO<sub>2</sub> Directly from a Carboxylate (A) or from a Tautomer of a Carboxylic Acid (B)



interesting variant of this pattern occurs in the neutral aqueous decarboxylation of  $\alpha,\beta$ -unsaturated carboxylic acids. In that process, a minor reactive tautomer, with a proton added  $\alpha$  to the carboxylate, provides a site that accepts electron density as CO<sub>2</sub> forms from the carboxylate (Scheme 1B).<sup>1,3</sup> While aromatic carboxylic acids are formally analogous to  $\alpha,\beta$ -unsaturated acids, they undergo decarboxylation in solution much more slowly, presumably because formation of the required tautomeric intermediate that is analogous to that in Scheme 1B involves loss of aromaticity.<sup>4–12</sup>

Hay and Taylor reported that the decarboxylation of 2,4-dimethoxybenzoic acid (**1**; Scheme 2) is subject to acid catalysis.<sup>5</sup> Based on a very limited data set and the already suspect Hammett-Zucker hypothesis,<sup>13–16</sup> they proposed a mechanism involving decarboxylation through the ring-protonated intermediate (**1H**<sup>+</sup>; Scheme 2). Schubert and co-workers reported a detailed kinetic analysis of the decarbox-

## Scheme 2. Decarboxylation of **1** through the Ring-Protonated Intermediate **1H**<sup>+</sup>



ylation of the closely related 2,4,6-trimethoxybenzoic acid.<sup>17</sup> They note the possibility of diverse formal mechanisms that are consistent with their results, including one that produces protonated CO<sub>2</sub> (HCO<sub>2</sub><sup>+</sup>). While this could apply to the reaction of **1** as well, the involvement of such a species in a reaction would be problematic as the proton affinity of CO<sub>2</sub> is so low that its conjugate acid is not an accessible component of a transition state.<sup>3,18</sup> This can be appreciated from the recent report of Reed and co-workers.<sup>19</sup> Treatment of CO<sub>2</sub> with an unusually powerful Brønsted acid produces the dimeric form of protonated CO<sub>2</sub>: H(CO<sub>2</sub>)<sub>2</sub><sup>+</sup>. Even under those extreme conditions, there is “no evidence for the presence of the HCO<sub>2</sub><sup>+</sup> ion” itself.<sup>19</sup> This implies that alternative pathways that avoid HCO<sub>2</sub><sup>+</sup> would be significantly lower in energy and more accessible.

In order to clarify the nature of the catalytic process for the decarboxylation of **1**, we examined the rate of the reaction over a range of acidity that includes the apparent pK<sub>A</sub> for formation of the conjugate acid of **1**. The results permit the detailed consideration of the role of acidity in promoting decarboxylation.

Received: February 17, 2016

Published: May 31, 2016

## RESULTS

The first-order rate constants for the decarboxylation of **1** at 60 °C are plotted as a function of the Hammett acidity function ( $H_0$ ) in Figure 1 (data are in Table S1; Supporting

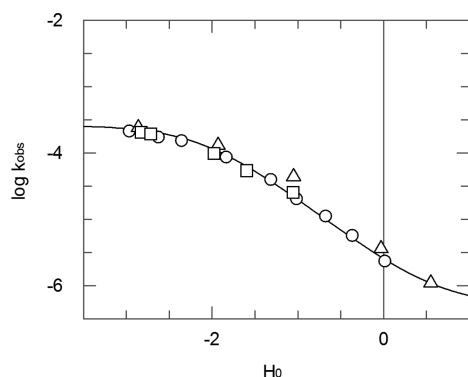


**Figure 1.** Logarithm of the first-order rate constants for the decarboxylation of **1** at 60 °C as a function of Hammett acidity function values ( $H_0$ ) for perchloric acid (O), sulfuric acid (□), and hydrochloric acid (Δ) solutions. Data are fit to the equation of a titration curve with an apparent  $pK_A$  of  $-2.1$ . This dependence in its simplest form fits a reaction process involving the neutral and protonated forms of the reactant (Scheme 3), with the protonated form reacting more rapidly.

Information). The results are consistent with the limited data reported by Hay and Taylor for solutions of equivalent acidity as measured by  $H_0$ .<sup>5</sup> The observed first order rate constants for the decarboxylation of **1** as a function of acidity give a reasonable fit to the equation of a titration curve for an acid with a  $pK_A = -2.1$ . Since the  $H_0$  values are based on the protonation equilibria of aniline derivatives,<sup>20</sup> we expect some deviation from a precise fit. The rate of reaction increases with the acidity of the medium, independent of the conjugate base of the mineral acid, establishing that the reaction depends only on the protonating power of the medium itself and that there are no differential effects from these weak Brønsted bases. The rates in the more acidic regions of the plot (at  $H_0 < -2.5$ ) are trending toward becoming independent of acidity, consistent with the rate being dependent upon the formation of the conjugate acid of **1**.

$$k_{\text{obs}} = k_0 + k_{\text{H}^+}(\mathbf{1}[\text{H}^+]) / (K_A + [\text{H}^+]) \quad (1)$$

The logarithmic curve for the dependence of  $k_{\text{obs}}$  on acidity (eq 1) will fit the macroscopic  $pK_A$  of  $[\mathbf{1}\text{H}^+]$ . We expect that the actual reactive species in the two processes will be tautomers of the macroscopically titrating species; therefore, the dependence of rate on acidity will fit the same curve.

The  $pK_A$  values for the conjugate acids of benzoic acid and for 4-methoxybenzoic acid are  $-4.39$  and  $-3.95$ , respectively.<sup>21</sup> The additional methoxy substituent in **1** should have a cumulative effect that is equal or less than that of the single methoxy group, giving an expected  $pK_A$  of around  $-3.5$ . Furthermore, the methoxy group ortho to the carboxyl group of **1** should stabilize the conjugate acid of the carboxyl through intramolecular hydrogen bonding. Stewart and Granger demonstrated that this type of interaction will increase the  $pK_A$  by about one unit.<sup>22</sup> The resulting estimated  $pK_A$  of  $-2.5$  is in reasonable agreement with the value obtained from our data plot ( $pK_A = -2.1$ ). Schubert and co-workers fit their kinetic data for the decarboxylation of 2,4,6-trimethoxybenzoic

acid to a  $pK_A$  of  $-0.9$  for the conjugate acid at the carboxyl. They attribute the perturbed basicity to stabilization of the protonated carboxyl group through its H-bonding to the adjacent methoxy groups.<sup>17</sup> The median value between the  $pK_A$  for the 4-methoxy and 2,4,6-trimethoxy benzoic acid should roughly approximate the  $pK_A$  of **1**. Indeed, the estimate of  $-2.4$  is likewise consistent with the  $pK_A$  of  $-2.1$  obtained from fitting the observed first order rate constants for the decarboxylation of **1**.

**Experimental Test of Actual vs Apparent  $pK_A$ .** In order to determine independently whether the apparent  $pK_A$  in Figure 1 corresponds to the conjugate acid of **1**, we titrated a solution of **1** using perchloric acid, dissolved in acetic acid and water, in the presence of the Hammett base 2-nitroaniline. Spectral changes will occur upon addition of a species that can function as a Brønsted base with respect to the indicator in the solution.<sup>23</sup> The AcOH/ $\text{H}_2\text{O}$ / $\text{HClO}_4$  system is advantageous as it allows access to very acidic conditions (with negative  $H_0$  values) at low acid concentrations.<sup>23</sup> Using this method, the addition of a small quantity of **1** is sufficient to shift the equilibrium upon protonation. Using this system, we determined the  $pK_A$  of the conjugate acid of **1** to be about  $-2.5$ . Error associated with this value is moderate, as the absorbance changes of the indicator are small. However, this value is consistent with both the estimated acidity of **1** and the apparent  $pK_A$  from the  $H_0$ -rate profile. We also validated the approach with a positive control using DMSO as the potential base. The observed  $pK_A$  of the conjugate acid of DMSO is  $-1.70$ , which agrees with reported values.<sup>24</sup> These results support the conclusion that the dependence of the observed rates of decarboxylation of **1** on the acidity of the medium is the result of formation of a conjugate acid of **1**.

**Solvent Kinetic Isotope Effect with Acidity.** The observed first order rate constants for the decarboxylation of **1** in protonated and deuterated acid solutions are presented in Table 1. Uncertainties for these values are all in the second

**Table 1. Solvent Kinetic Isotope Effects for the Decarboxylation of **1** at Various Acidities at 60 °C**

$H_0$	$k_{\text{H}_2\text{O}} (\times 10^5 \text{ s}^{-1})$	$k_{\text{D}_2\text{O}} (\times 10^5 \text{ s}^{-1})$	$k_{\text{H}_2\text{O}}/k_{\text{D}_2\text{O}}$
$-2.82^a$	20.0	15.1	1.3
$-2.71^a$	19.0	14.1	1.3
$-1.97^a$	9.6	6.6	1.4
$-1.59^a$	5.3	3.6	1.5
$-1.05^a$	2.5	1.5	1.7
$0.55^b$	0.11	0.082	1.3

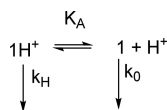
<sup>a</sup>Values determined with  $\text{D}_2\text{SO}_4$  and  $\text{H}_2\text{SO}_4$ . <sup>b</sup>Values determined with DCl and HCl.

decimal place. The very small solvent kinetic isotope effect at  $H_0 = 0.55$  suggests that the rate-limiting process for the uncatalyzed reaction that predominates at low acidity does not involve a kinetically significant proton transfer, with C–C bond cleavage from a neutral zwitterion being rate-limiting. However, at  $H_0 = -1.05$ , where the rate increases with acidity, the magnitude of the SKIE is more substantial. At higher acidity ( $H_0 < -2.5$ ), where the rate begins to plateau, the SKIE once again begins to decrease, consistent with rate determining C–C bond cleavage.

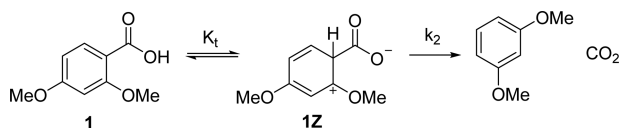
## DISCUSSION

**Decarboxylation of 1 under Neutral Conditions.** The curvature in Figure 1 that occurs at around  $H_0 = 0.5$  suggests a neutral mechanism for the decarboxylation of 1 that is independent of the acidity of the medium. The data in Figure 1 are fit with an apparent first order rate constant of  $5 \times 10^{-7} \text{ s}^{-1}$  for the neutral pathway. This decarboxylation is likely to proceed via tautomerization of 1 to a zwitterionic intermediate (1Z) and direct loss of  $\text{CO}_2$  from this species (Scheme 4).

**Scheme 3. Kinetic Scheme for Acid Catalysis via the Conjugate Acid of 1**



**Scheme 4. Neutral Mechanism for the Decarboxylation of 1 Proceeds through a Minor Tautomer (1Z)**



Considering the values of the  $\text{p}K_{\text{A}}$  for C4-protonated 1,3-dimethoxybenzene ( $\text{p}K_{\text{A}} \sim -9$ )<sup>25,26</sup> and for the carboxylic acid of 1 ( $\text{p}K_{\text{A}} \sim 4$ ),<sup>27</sup> we suggest that the rate constant for decarboxylation of the tautomer ( $k_2$ ) will be  $10^{13}$  times larger than the observed first order rate constant for the neutral reaction ( $k_2 \sim 10^6 \text{ s}^{-1}$ ). This approximation assumes that the effect of the carboxyl group on the acidity of the protonated 1,3-dimethoxybenzene is small.

**Deprotonation of COOH Concerted with Decarboxylation.** The decarboxylation of  $1\text{H}^+$  with concerted deprotonation of the COOH group by water (Scheme 5) is consistent with our results. Generally, concerted processes occur where the corresponding stepwise process is energetically inaccessible.<sup>28</sup> The ionization of the carboxyl group to the ring-protonated zwitterion is not likely to occur under the strongly acidic conditions employed in this study. Conversely, decarboxylation without proton transfer from the carboxyl group would produce  $\text{HCO}_2^+$ , which, as we have noted earlier, is not an energetically accessible species under any conditions.<sup>3,18,19</sup> Considering the energies of the “corners” of the corresponding More O’Ferrall diagram (Figure 2), the lowest energy transition state is likely to occur with nearly complete transfer of the carboxyl proton to water, thereby minimizing the extent of  $\text{HCO}_2^+$  character in the transition state for C–C cleavage.

The observed first order rate constants are generally independent of the identity of the conjugate base of the

**Scheme 5. Decarboxylation of  $1\text{H}^+$  May Occur with Concerted Deprotonation of the Carboxyl Group; the Associated Transition State Would Involve a Very Early Proton Transfer to Solvent Water**

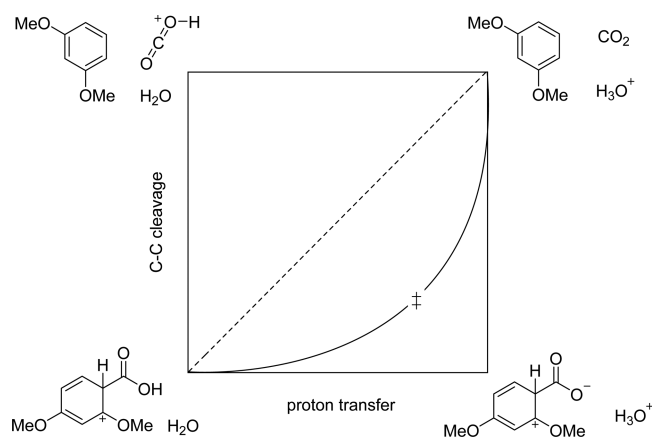
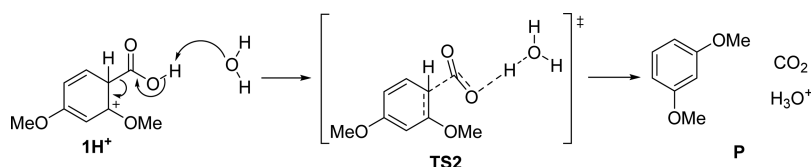


**Figure 2. Qualitative More O’Ferrall diagram for the formation of  $\text{CO}_2$  and 1,3-dimethoxybenzene from C1-protonated 1. The likely transition state ( $\ddagger$ ) involves considerable proton transfer and little C–C bond cleavage.**

dissolved acid as we expect water to have an overwhelming effect. A notable exception is that at some acidities,  $k_{\text{obs}}$  is larger for solutions made from HCl. This could arise from a specific effect of chloride ion in the transition state, facilitating transfer of the proton from the carboxyl to water. However, there is no deviation at  $H_0 \sim -3$ , where chloride concentration is highest. Therefore, we conclude that the deviations are a consequence of the imperfect match of the Hammett bases and 1.

**Consideration of a Hydrolytic Mechanism Producing Carbonic Acid.** Bender and co-workers reported that the addition of water to a carboxyl group is acid-catalyzed. They determined the rates of exchange from  $\text{H}_2^{18}\text{O}$  into the carboxyl of 4-methoxybenzoic acid at low acidity.<sup>29</sup> While those experiments were performed in dioxane–water mixtures at  $80^\circ\text{C}$ , the observed rate constant of  $6.4 \times 10^{-6} \text{ s}^{-1}$  at  $H_0 \sim 1.4$  suggests that hydration of 1 would be a kinetically competent step at the higher acidities employed in our study. Though hydration does not necessarily occur along the decarboxylation pathway, hydrated species are potentially viable intermediates (Scheme 6) on the route to carbonic acid.

Ring protonation at C1 would also be necessary for decarboxylation from the hydrate ( $1\text{H}^+$ ). Decomposition of this species would likely involve C–C bond cleavage and concerted deprotonation of the departing carbonic acid. We find that consideration of the corresponding stepwise process with a More O’Ferrall diagram (Figure 3) is highly informative. As discussed above, deprotonation prior to decarboxylation would produce a zwitterionic alkoxide. This is unlikely to occur under the acidic reaction conditions. Direct C–C bond cleavage without proton transfer would produce protonated carbonic acid (PCA). While this species is considerably more stable than  $\text{HCO}_2^+$ ,<sup>30–32</sup> a pathway involving concerted proton transfer will produce carbonic acid and will likely be lower in

**Scheme 6. Decarboxylation from the Ring-Protonated Hydrate ( $1'H^+$ ) with Concerted Proton Transfer Would Produce Carbonic Acid, Which forms  $CO_2$  Rapidly**

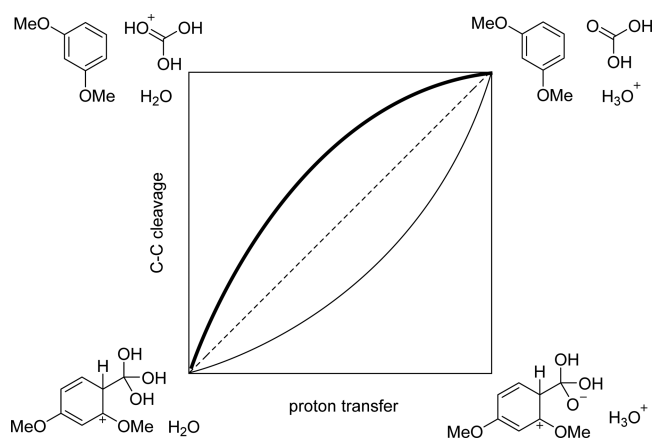
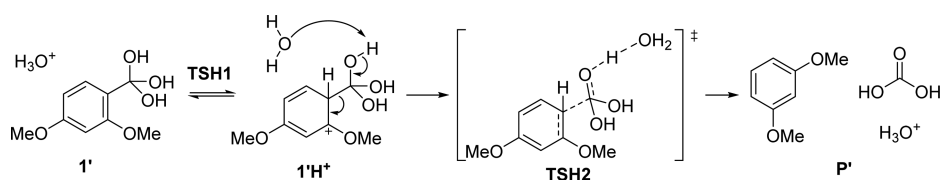


**Figure 3.** Qualitative More O'Ferrall diagram for formation of carbonic acid and 1,3-dimethoxybenzene from  $1'H^+$ . Potential routes include concerted pathways with early proton transfer (plain curve), early C–C bond cleavage (bold curve), or synchronous C–C cleavage and proton transfer (dashed line).

energy. As PCA is not nearly as unstable as  $HCO_2^+$ , the transition state for this process (depicted in Scheme 6) should include a more symmetrical proton transfer. However, the basis for synchronicity of C–C bond cleavage and proton transfer is not immediately clear in this instance. Reactions proceeding with early C–C bond cleavage (bold curve in Figure 3) and early deprotonation (plain curve in Figure 3) are both reasonable. Intuitively, the species in the top-left corner of Figure 3 will be lower in energy under the highly acidic reaction

conditions and the corresponding transition state will have C–C bond cleavage more advanced than proton-transfer.

**Computational Analysis of the Potential Mechanisms of Decarboxylation.**

We have noted that the acid-catalyzed decarboxylation of **1** might proceed through the ring protonated carboxylic acid ( $1H^+$ ) or the ring protonated hydrate ( $1'H^+$ ). These mechanisms would be indistinguishable from kinetic measurements (since the concentration of water is not in the observed rate law). Therefore, we used computational methods to evaluate the relative energies of the potential pathways. Structures were optimized at the M06-2X/6-311++G(2d,2p) level of theory with two common implicit solvent models: SMD<sup>33</sup> and PCM.<sup>34</sup> We used two distinct solvation models in order to assess the generality of the results. While SMD generally gives more accurate free energies of solvation for complex species in water,<sup>35,36</sup> we do not assume that the absolute energies of solvation are precise from applying either model alone. The stabilities of charged species studied here are likely to be underestimated by gas-phase calculations that use implicit solvation models. While our calculations were performed with one or two explicitly modeled water molecules, this will not describe the effects of bulk solvation accurately. Instead, we assume that errors in solvation energies are roughly equal for all charged species, such that the qualitative trends in the computed free energies of the compounds can be used to distinguish between the two reaction pathways.

The resulting reaction profiles (Figure 4) reveal that the decarboxylation of **1** proceeds through  $1H^+$ . The hydrate (**1'**) is also energetically accessible and we are able to locate a transition state for its C–C cleavage to produce carbonic acid (as illustrated in Figure 3). However, regardless of the solvation

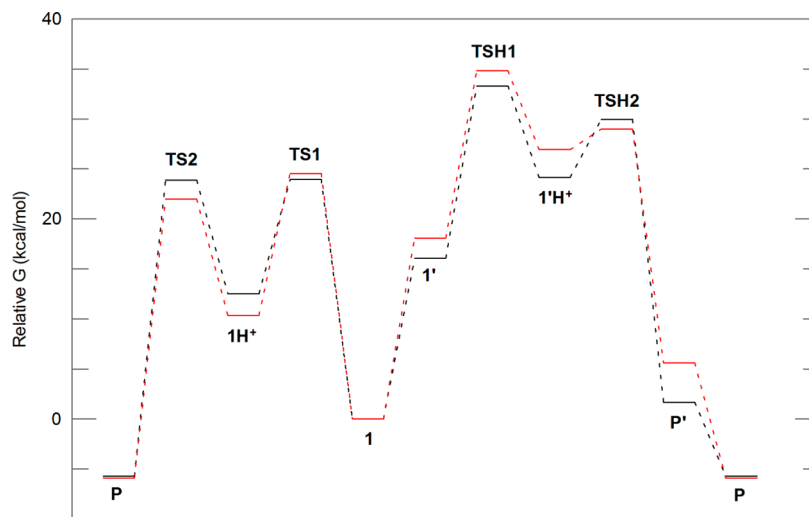


**Figure 4.** Computed reaction profiles for the decarboxylation of **1** through the loss of  $CO_2$  and the loss of carbonic acid. Labels refer to structures in Schemes 2 and 6. All computations were performed at the M06-2X/6-311++G(2d,2p) level with two water molecules (see Experimental Section). Bulk solvation was considered implicitly with the SMD (black) and PCM (red) models.



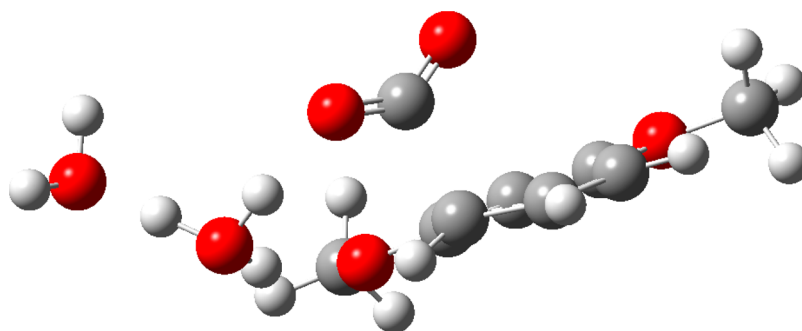


**Figure 5.** Computed TS for decarboxylation of  $1\text{H}^+$  shows nearly no  $\text{HCO}_2^+$  character. Vibrational analysis confirms that deprotonation of the  $\text{COOH}$  is concerted with  $\text{C}-\text{C}$  bond cleavage. This structure was optimized with M06-2X/6-311++G(2d,2p)//SMD.

model used, the free energy barrier for the hydrolytic process is about 10 kcal/mol higher than that for the corresponding loss of  $\text{CO}_2$  from  $1\text{H}^+$  with requisite concerted transfer of the carboxyl proton to water (as in Figure 2). Proton transfer from the carboxyl of  $1\text{H}^+$  to water is nearly complete at the transition state for  $\text{C}-\text{C}$  cleavage, such that there is essentially no  $\text{HCO}_2^+$  character in that transition state (see Figure 5). In contrast, the transition state for product formation from  $1'\text{H}^+$  shows little transfer of the proton from the departing carbonic acid derivative to water, though vibrational analysis indicates that this proton transfer occurs along the  $\text{C}-\text{C}$  bond cleavage reaction coordinate (see Figure 6). This difference in the

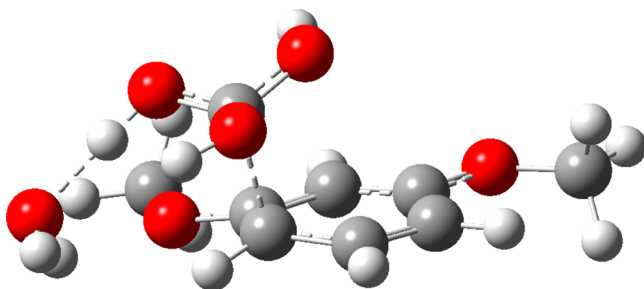


**Figure 6.** Optimized TS for the loss of carbonic acid from  $1'\text{H}^+$  shows a small degree of proton transfer from departing PCA to solvent water. This structure was computed using M06-2X/6-311++G(2d,2p)//SMD.

synchronicity of the proton transfer reflects the stability of protonated carbonic acid (PCA) relative to that of  $\text{HCO}_2^+$ . While PCA is much more stable than  $\text{HCO}_2^+$ , the computed transition state indicates that release of neutral carbonic acid is a more efficient process. This suggests that instances involving decarboxylation through formation of a hydrate and protonated carbonic acid<sup>6-9</sup> should involve concerted deprotonation as an additional feature (or may proceed via loss of  $\text{CO}_2$  and proton transfer).

## CONCLUSIONS

The acceleration of decarboxylation of certain benzoic acids in acidic solutions is associated with the presence of substituents that promote protonation on the benzene ring adjacent to the carboxyl group. However, the macroscopic protonation of the reactant occurs on the carboxyl, with the reactive species being a minor tautomer that is not aromatic. This intermediate cannot decompose by  $\text{C}-\text{C}$  bond cleavage alone, as that would produce the energetically prohibitive conjugate acid of  $\text{CO}_2$ . Our kinetic analysis reveals that the rate of the overall reaction

follows the titration curve for converting the reactant to the conjugate acid but does not reveal how that process leads to the formation of the observed products. Our computational results allow us to conclude that the  $\text{C}-\text{C}$  bond cleavage step occurs together with transfer of the carboxyl proton to water, forming  $\text{CO}_2$  and  $\text{H}_3\text{O}^+$  along 1,3-dimethoxybenzene. Alternative mechanisms, via hydration of the carboxyl and ring protonation to produce carbonic acid and  $\text{H}_3\text{O}^+$ , avoid forming protonated  $\text{CO}_2$  but the combination of hydration and protonation adds an additional barrier that leads to a less efficient outcome than is achieved without hydrate formation.

## EXPERIMENTAL SECTION

**Kinetics of the Decarboxylation of 2,4-Dimethoxybenzoic Acid.** 2,4-Dimethoxybenzoic acid and 1,3-dimethoxybenzene were obtained from commercial suppliers and used without purification. All solutions were prepared with reagent-grade hydrochloric acid, sulfuric acid, or perchloric acid in doubly distilled, deionized water. The rate of decarboxylation of 2,4-dimethoxybenzoic acid was measured in solutions of hydrochloric acid, sulfuric acid and perchloric acid of  $H_0$ -defined acidity. Solvent kinetic isotope effects were obtained using solutions of deuterated sulfuric acid or hydrochloric acid in  $\text{D}_2\text{O}$ . Reaction progress was monitored by the decrease in absorbance at 260 nm using a double beam UV-vis spectrometer. The cell compartment was maintained at  $60^\circ \pm 0.1^\circ \text{C}$  using an interfaced Peltier thermostat. Data were collected with an interfaced computer and the first-order rate constants were obtained by nonlinear regression analysis with GraFit 6 (Erithacus Software). Under conditions where the reaction is exceedingly slow, we used the method of initial rates to obtain the values of the observed first-order rate constants for those conditions.

**Measurement of the  $pK_A$  of the Conjugate Acid of 1.** We followed the established procedure as described by Wiberg and Evans. The  $pK_A$  of the Hammett base 2-nitroaniline was determined spectrophotometrically at  $60^\circ \text{C}$  using HCl solutions of known  $H_0$  values at this temperature. This value ( $pK_A = -0.49$ ) was used to determine the  $H_0$  values of mixtures of perchloric acid in acetic acid and water in the usual manner.<sup>37</sup> 5.0 g of a 1.6 M perchloric acid solution was added to 90 mL of glacial acetic acid. Approximately 3 mg of 2-nitroaniline was then added to that solution. The  $H_0$  value of this mixture at  $60^\circ \text{C}$  was determined to be  $-0.48$ . Portions of this mixture were dispensed into quartz cuvettes. Where an added substance becomes protonated in the perchloric acid/acetic acid/water mixture, the concentration of the free base of 2-nitroaniline will increase. The magnitude of the corresponding increase in absorbance at 400 nm can then be used to calculate the  $pK_A$  of the conjugate acid of the added substance. The change in the absorbance of a 0.05 M solution of 1 indicates that the  $pK_A$  of the conjugate acid of 1 is approximately  $-2.5$ . As a control, the absorbance of a 0.05 M solution of DMSO in the described perchloric acid solution was recorded. The increase in absorbance at 400 nm relative to the blank indicates that the  $pK_A$  of the conjugate acid of DMSO is  $-1.70$ . This is in good agreement with literature values.<sup>24</sup> As a negative control, a 0.05 M solution of 1,3-

dimethoxybenzene in the  $H_0 = -0.48$  mixture was prepared. As expected, the absorbance at 400 nm is unchanged relative to the blank solution.

**Computational Methodology.** All geometry optimizations and frequency calculations were performed with M06-2X/6-311++G-(2d,2p) as implemented in Gaussian 09.<sup>38</sup> As the hydrolytic mechanism involves the direct participation of  $H_3O^+$  and  $H_2O$ , all structures were optimized in the presence of two explicit molecules of water. For each structure, the protonation state of the water molecules was modified according to the proposed mechanistic scheme. Further solvation effects were considered implicitly with a self-consistent reaction field (SCRF) with the SMD or PCM solvation models.<sup>33</sup> The identity of stationary points was confirmed through vibrational analysis. Intrinsic reaction coordinate (IRC) calculations were used to evaluate the identities of located transition states. Free energy values used in the construction of the reported potential energy surface were obtained from frequency calculations performed at 60 °C using the recommended scaling factor of 0.97.<sup>39</sup>

## ■ ASSOCIATED CONTENT

### Supporting Information

The Supporting Information is available free of charge on the ACS Publications website at DOI: 10.1021/jacs.6b01770.

Full citation for ref 38; rate constants used to construct Figure 1; coordinates and thermodynamics of all optimized structures. (PDF)

## ■ AUTHOR INFORMATION

### Corresponding Author

\*r.kluger@utoronto.ca

### Author Contributions

†G.W.H. and A.A.V. contributed equally.

### Notes

The authors declare no competing financial interest.

## ■ ACKNOWLEDGMENTS

This work was supported by NSERC Canada through a Discovery Grant to R.K. and postgraduate scholarship to G.W.H. Our computational studies were made possible by the facilities of the Shared Hierarchical Academic Research Computing Network (SHARCNET) and Compute/Calcul Canada. Dedicated to the memory of Robin A. Cox (1943–2015).

## ■ REFERENCES

- (1) Kluger, R. *Pure Appl. Chem.* **2015**, *87*, 353.
- (2) Kluger, R. *Acc. Chem. Res.* **2015**, *48*, 2843.
- (3) Guthrie, J. P. *Bioorg. Chem.* **2002**, *30*, 32.
- (4) Dunn, G. E.; Lee, G. K. *Can. J. Chem.* **1971**, *49*, 1032.
- (5) Hay, R. W.; Taylor, M. J. *Chem. Commun.* **1966**, 525.
- (6) Vandersteen, A. A.; Mundle, S. O. C.; Lacrampe-Couloume, G.; Sherwood Lollar, B.; Kluger, R. *J. Org. Chem.* **2013**, *78*, 12176.
- (7) Vandersteen, A. A.; Mundle, S. O. C.; Kluger, R. *J. Org. Chem.* **2012**, *77*, 6505.
- (8) Mundle, S. O. C.; Lacrampe-Couloume, G.; Lollar, B. S.; Kluger, R. *J. Am. Chem. Soc.* **2010**, *132*, 2430.
- (9) Mundle, S. O. C.; Kluger, R. *J. Am. Chem. Soc.* **2009**, *131*, 11674.
- (10) Schubert, W. M. *J. Am. Chem. Soc.* **1949**, *71*, 2639.
- (11) Longridge, J. I.; Long, F. A. *J. Am. Chem. Soc.* **1968**, *90*, 3092.
- (12) Johnson, W. S.; Heinz, W. E. *J. Am. Chem. Soc.* **1949**, *71*, 2913.
- (13) Zucker, L.; Hammett, L. P. *J. Am. Chem. Soc.* **1939**, *61*, 2791.
- (14) Hammett, L. P. *Physical Organic Chemistry*; McGraw-Hill Inc.: New York, 1940. (Reinterpretation in second edition, page 286.)
- (15) Bunnett, J. F. *J. Am. Chem. Soc.* **1961**, *83*, 4978.
- (16) Bunnett, J. F.; Olsen, F. P. *Can. J. Chem.* **1966**, *44*, 1917.

- (17) Schubert, W. M.; Zahler, R. E.; Robins, J. *J. Am. Chem. Soc.* **1955**, *77*, 2293.
- (18) Traeger, J. C.; Kompe, B. M. *Org. Mass Spectrom.* **1991**, *26*, 209.
- (19) Cummings, S.; Hratchian, H. P.; Reed, C. A. *Angew. Chem., Int. Ed.* **2016**, *55*, 1382.
- (20) Hammett, L. P.; Deyrup, A. J. *J. Am. Chem. Soc.* **1932**, *54*, 2721.
- (21) De Maria, P.; Fontana, A.; Spinelli, D.; Dell'Erba, C.; Novi, M.; Petrillo, G.; Sancassan, F. *J. Chem. Soc., Perkin Trans. 2* **1993**, *2*, 649.
- (22) Stewart, R.; Granger, M. R. *Can. J. Chem.* **1961**, *39*, 2508.
- (23) Wiberg, K. B.; Evans, R. J. *J. Am. Chem. Soc.* **1958**, *80*, 3019.
- (24) Landini, D.; Modena, G.; Scorrano, G.; Taddei, F. *J. Am. Chem. Soc.* **1969**, *91*, 6703.
- (25) Kresge, A. J.; Chen, H. J.; Hakka, L. E.; Kouba, J. E. *J. Am. Chem. Soc.* **1971**, *93*, 6174.
- (26) Kresge, A. J.; Mylonakis, S. G.; Sato, Y.; Vitullo, V. P. *J. Am. Chem. Soc.* **1971**, *93*, 6181.
- (27) Srivastava, K. C. *Bull. Chem. Soc. Jpn.* **1966**, *39*, 1591.
- (28) Jencks, W. P. *Acc. Chem. Res.* **1980**, *13*, 161.
- (29) Bender, M. L.; Stone, R. R.; Dewey, R. S. *J. Am. Chem. Soc.* **1956**, *78*, 319.
- (30) Olah, G. A.; Laali, K. K.; Wang, Q.; Prakash, G. K. S. *Onium Ions*; John Wiley & Sons: New York, 1998.
- (31) Olah, G. A. *Angew. Chem., Int. Ed. Engl.* **1993**, *32*, 767.
- (32) Olah, G. A.; White, A. M. *J. Am. Chem. Soc.* **1968**, *90*, 1884.
- (33) Marenich, A. V.; Cramer, C. J.; Truhlar, D. G. *J. Phys. Chem. B* **2009**, *113*, 6378.
- (34) Scalmani, G.; Frisch, M. J. *J. Chem. Phys.* **2010**, *132*, 114110.
- (35) Guthrie, J. P. *J. Phys. Chem. B* **2009**, *113*, 4501.
- (36) Marenich, A. V.; Cramer, C. J.; Truhlar, D. G. *J. Phys. Chem. B* **2009**, *113*, 4538.
- (37) Paul, M. A.; Long, F. A. *Chem. Rev.* **1957**, *57*, 1.
- (38) Frisch, M. J. et al. *Gaussian 09*; Gaussian, Inc.: Wallingford, CT, 2009.
- (39) Alecu, I. M.; Zheng, J.; Zhao, Y.; Truhlar, D. G. *J. Chem. Theory Comput.* **2010**, *6*, 2872.